# Numerical modeling of the September 13, 1999 landslide and tsunami on Fatu Hiva Island (French Polynesia)

Hélène Hébert, Alessio Piatanesi,[1] Philippe Heinrich, and François Schindelé
Laboratoire de Détection et de Géophysique, CEA, Bruyères-le-Châtel, France

Emile A. Okal
Department of Geological Sciences, Northwestern University, Evanston, Illinois, USA

Received 12 July 2001; accepted 5 October 2001; published 31 May 2002.

[1] On September 13, 1999, Omoa Bay (Fatu Hiva Island, French Polynesia) was struck by 2 to 5 m high water waves: several buildings were flooded and destroyed but no lives were lost. Observations gathered during a post-event survey revealed the recent collapse into the sea of a $300 \times 300$ m$^2$, at least 20-m thick, cliff located 5 km southeast of Omoa. This cliff failure most certainly triggered the tsunami waves since the cliff was reported intact 45 min earlier. We simulate the tsunami generation due to a subaerial landslide, using a finite-difference model assimilating the landslide to a flow of granular material. Numerical modeling shows that a 0.0024-km$^3$ landslide located in the presumed source area accounts for the tsunami waves reported in Omoa Bay. We show that the striking amplification observed in Omoa Bay is related to the trapping of waves due to the shallow submarine shelf surrounding the island. *INDEX TERMS:* 3020 Marine Geology and Geophysics: Littoral processes; 4255 Oceanography: General: Numerical modeling; 4564 Oceanography: Physical: Tsunamis and storm surges; 9355 Information Related to Geographic Region: Pacific Ocean

## 1. Introduction

[2] On September 13, 1999, at 22:45 UTC (13:15 local time) two successive 2- to 5-m high seawaves struck the shore of Omoa Bay on Fatu Hiva Island (Marquesas Islands, French Polynesia) (Figure 1). In particular, they flooded several rooms at the local school, smashing windows and depositing up to 25 cm of sand in the teachers' office. Fortunately, the principal and teachers managed to evacuate the pupils out of the classroom just before the second (and larger) wave, so that a disaster was avoided and no injuries resulted. A nearby concrete building was severely damaged. This event was also observed in Hanavave Bay, 4 km to the north of Omoa, but here maximal water height did not exceed 1.9 m. Due to their particular coastal shape, the Marquesas Islands are prone to local amplification in response to tsunamis generated by earthquakes occuring at the Pacific Rim [*Guibourg et al.*, 1997; *Heinrich et al.*, 1998a; *Hébert et al.*, 2001]. However neither a Pacific-wide tsunami nor wave observations on tide gages available in French Polynesia were reported on that day, and thus the event was quickly identified as being of local origin, with very localized damage.

[3] On the following morning, local residents discovered a major fresh landslide along a cliff located about 5 km from Omoa. As seen on a photograph (Figure 2) taken three weeks later during the post-event survey organized by four members of the International Tsunami Survey Team [*Fryer et al.*, 2000; *Okal et al.*, The landslide and tsunami of 13 September 1999 in Fatu Hiva (Marquesas, French Polynesia), submitted to *Bull. Soc. Géol. France*, 2001], the slide is at least 300-m high by 300-m wide. A key report by a local fisherman stated that the cliff was intact as of 12:30 local time, indicating beyond doubt that the landslide caused the tsunami and the waves in Omoa Bay.

[4] In this paper we provide a numerical modeling of the 1999 Fatu Hiva landslide and tsunami, using a method which was recently applied successfully to model subaerial or submarine mass slumps, some of them followed by tsunamis [*Heinrich et al.*, 1998b, 2000, 2001a, 2001b]. We show that a subaerial 0.0024 km$^3$ landslide, initiated in the area of the cliff failure, can trigger a tsunami reaching Omoa Bay 4 minutes later and producing 2- to 5-m high water waves. We discuss this result and stress the influence of the local submarine bathymetry on the coastal trapping of tsunami waves.

## 2. Model and Data

### 2.1. Landslide

[5] We assume that the body of rock suddenly loses its equilibrium and slides downslope under gravity forces. The landslide is treated as a fluid-like flow of granular material, following the approach proposed by *Savage and Hutter* [1989]. The slide thickness is much smaller than the characteristic slide length, thus mass and momentum conservation equations are depth-averaged over the thickness: this allows us to ignore the precise mechanical behavior within the flow. The deformation is assumed to be essentially located in a thin boundary layer near the bed surface. Energy dissipation is then neglected within the flow and is limited to basal friction modeled by a Coulomb-type friction law. This law is similar to a friction law for a rigid block on an inclined plane; it assumes a constant ratio of the shear stress to the normal stress at the base and involves a dynamic friction angle $\varphi$ between the rough bed and the mass.

[6] Our approach of a fluid-like flow is commonly used to model landslides considered as viscous flows [*Jiang and Leblond*, 1992; *Rabinovich et al.*, 1999; *Assier-Rzadkiewicz et al.*, 2000]. Arguably, the flow of a granular material may be inappropriate for a cliff failure, and a rigid body rock made of blocks possibly interacting with each other [*Tinti et al.*, 1999] may be more realistic. However it has to be noted that slide duration is short in our case, and that pressure forces due to height gradients are small compared to the gravity and to the Coulomb basal friction. Our method takes into account these two governing forces, and the resulting equations of mass (1) and momentum (2) conservation, written in a $(x, y)$ coordinate system linked to the topography, read:

$$\frac{\partial h}{\partial t} + \frac{\partial}{\partial x}(hu) + \frac{\partial}{\partial y}(hv) = 0 \qquad (1)$$

[1]Now at INGV, Roma, Italy.

Copyright 2002 by the American Geophysical Union.
0094-8276/02/2001GL013774$05.00

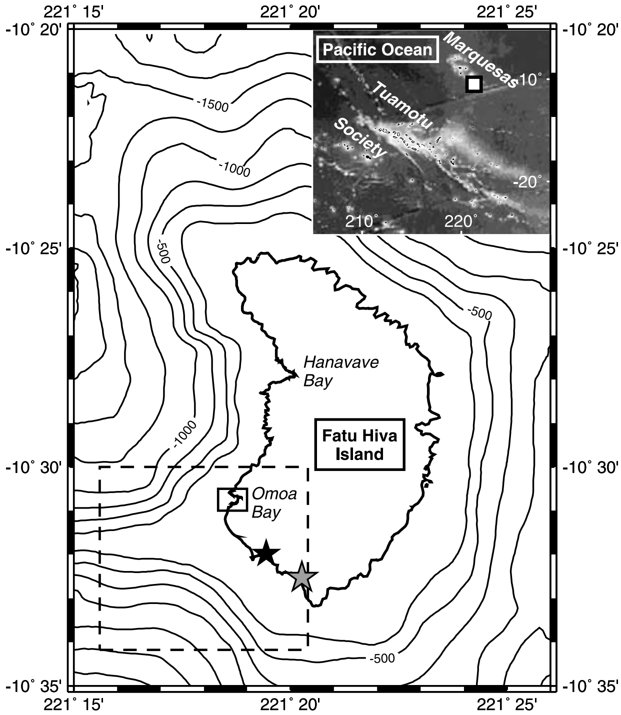


**Figure 1.** Bathymetric map around Fatu Hiva Island. Contours digitized from French hydrographic (SHOM) maps are displayed at 250 m intervals. The black star indicates the location of the subaerial landslide identified on Figure 2; the gray star indicates the location used for the additional computation, with the source shifted southeast. The computational domain is shown as the dashed box. Insert shows the location of the Marquesas Islands in the Pacific Ocean. Fatu Hiva Island is indicated by the white square.

$$\frac{\partial}{\partial t}(hu) + \frac{\partial}{\partial x}\left(hu^2\right) + \frac{\partial}{\partial y}(huv) = -\frac{1}{2}\kappa\frac{\partial}{\partial x}\left(gh^2\cos\theta\right) + \kappa gh\sin\theta_x + F_x$$

$$\frac{\partial}{\partial t}(hv) + \frac{\partial}{\partial x}(hvu) + \frac{\partial}{\partial y}\left(hv^2\right) = -\frac{1}{2}\kappa\frac{\partial}{\partial y}\left(gh^2\cos\theta\right) + \kappa gh\sin\theta_y + F_y \qquad (2)$$

with $\kappa = 1 - \rho_w/\rho_s$ and $\mathbf{F} = -\kappa\, gh \cos\theta\tan\varphi\mathbf{u}/\|\mathbf{u}\|$ where $\mathbf{u} = (u, v)$ is the depth-averaged velocity vector parallel to the bed, $h$ is the slide thickness perpendicular to the slope, $\rho_w$ and $\rho_s$ are the water and rock densities with a ratio $\rho_s/\rho_w = 2$, $\theta\ (x, y)$ is the local steepest slope angle, $\theta_x$ and $\theta_y$ are the slope angles along the $x$- and $y$-axes respectively.

### 2.2. Tsunami

[7] The shallow water model (long wave theory) can be applied to the tsunami as long as wavelengths remain much larger than the water depth. In our case we find that the wavelength/depth ratio is quite small (about 10) and characteristic dimensions of the slide are close to the water depth, implying probable dispersive effects in the propagation. We thus fall in the limit of the shallow water approximation. However the propagation duration is rather short (4 min) and corresponds to about 3 to 4 wavelengths, thus frequency dispersive effects remain small. In addition, numerical models similar to ours have been proved to deal properly with amplitude dispersive effects close to shore and due to shoaling effects, where the wave amplitudes become larger than the water depth [*Titov and Synolakis*, 1995].

[8] Equations governing the landslide and the tsunami propagation are similar and are thus solved using the same Godunov-type scheme, extended to second order by using the concept of Vanleer [*Alcrudo and Garcia-Navarro*, 1993; *Mangeney et al.*, 2000]. This model is particularly adapted to deal with nonlinear waves. The time history of seabottom deformation resulting from the landslide is introduced as a known forcing term $(\cos\theta)^{-1}\partial h/\partial t$ in the mass conservation equation of the tsunami model. Finally, our model also allows the computation of inundation (run-up) heights provided topographic data are available at the receiving shore.

### 2.3. Data

[9] Bathymetric data are required to model the propagation of the tsunami waves around the island. We digitized depth contours ranging from $-2000$ up to 0 m on map 7354 of the French Hydrographic Service (SHOM) (scale: 1:70000), with refined contours ranging from $-50$ to $-2$ m taken from the 1:10000 sketch around Omoa Bay. Topographic data must also be added in Omoa Bay in order to compute run-up heights. However such topographic data are not available up to now for Fatu Hiva Island, so we gathered observations reported and photographs taken during the post-event survey, allowing us to build contours from 0 to 10 m. The resulting $8 \times 7\text{-km}^2$ grid, with an about 20-m cell size, encompasses the cliff failure area and Omoa Bay (limits shown in Figure 1).

## 3. Results and Discussion

[10] In a first approach, two different initial volumes (0.0012 and 0.0024 $km^3$) were tested for a landslide located in the presumed source area. The friction angle was chosen as $\varphi = 30°$, consistent with cases of subaerial landslides [*Voight*, 1979]. Maximal water heights computed in Omoa Bay for the smallest initial volume range from 1 to 2 m in the bay (Figure 3b) and reach no more than 3 m close to the school location, not satisfactorily explaining the observed inundations. For the largest volume, Figure 3a displays maximal water heights computed in Omoa Bay after an 8-min propagation time. Values range from 1 to 5 m locally (about 4 m near the school) and the water penetration is observed to be 100 to 200 m inland. A numerical gage located in the bay shows that the first wave is a positive 3-m high wave reaching the bay after a 5-min propagation, followed about 2 minutes later by a second, 2.5 m, wave, with an about 2-min spacing in between. These results are in good agreement with eyewitness reports [*Fryer et al.*, 2000; *Okal et al.*, subm.]. In

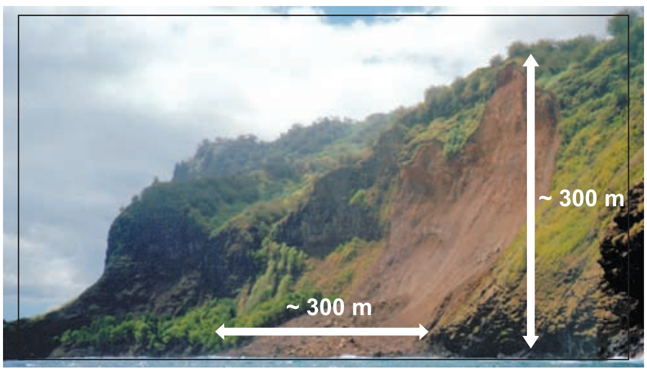


**Figure 2.** Photograph taken by the post-event survey team on Oct. 5, 1999, at the location indicated by the black star on Figure 1. The surface area involved in the cliff failure can be estimated as $300 \times 300\ m^2$.

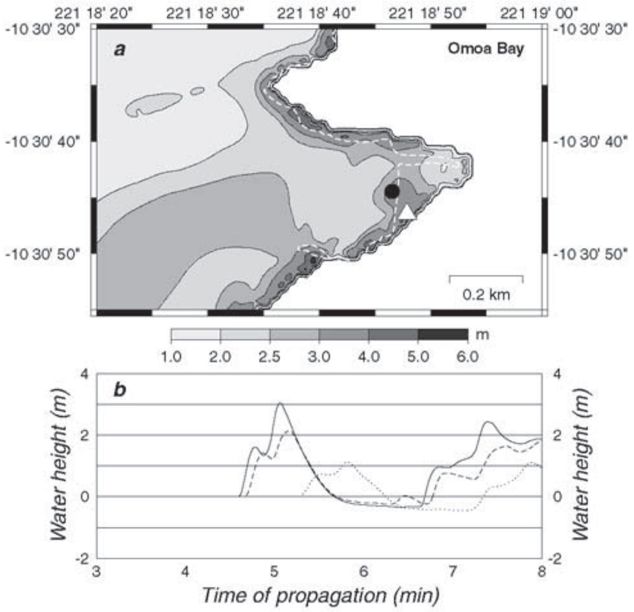


**Figure 3.** (a) Maximal water heights computed in Omoa Bay after an 8-min propagation are shown with 1-m contours. The dashed white line corresponds to the shoreline at rest. The white triangle displays the location of the school where waves at least 3-m high were reported. The numerical gage used during the computation is shown as the black disk. (b) Water heights obtained at this gage for the 0.0024-$km^3$ event simulation (solid line), the 0.0012-$km^3$ event simulation (dashed line), and the shifted 0.0024-$km^3$ event (dotted line) are plotted as a function of the propagation time.

addition, this modeling defines a realistic volume for the landslide that triggered the tsunami, suggesting a thickness of about 27 m (about 13 m for the smaller 0.0012 $km^3$ volume) for the $300 \times 300$ $m^2$ slide identified during the post-event survey.

[11] In order to investigate the behavior of tsunami waves around Fatu Hiva Island during the 1999 event, we plot the maximal water heights reached after an 8-min modeling time in the whole computational domain (Figure 4a). This map indicates the spatial distribution of the tsunami energy, and particularly the focusing towards Omoa Bay through a particular behavior of the waves. Indeed part of the energy seems to have been refracted about 2 km off shore and then redirected towards the coast. This corresponds to a trapping of the waves due to the seafloor topography: the area where submarine slopes are the steepest defines a narrow band that separates two domains with different mean water depths $h$ (less than 200 m and more than 1000 m), hence with contrasting wave velocities $c = (gh)^{1/2}$. The smaller 0.0012-$km^3$ event located at the same source provokes the same trapping and focusing, however with smaller amplitudes reaching Omoa Bay (Figure 3b and Figure 4b).

[12] These edge waves evidenced in our results are one type of topographically trapped waves that can be generated from any disturbance located close to shore [*Mysak*, 1980], and that propagate in a sloping domain. Whatever the slide volume, modelings underline the same trapping of the waves eastward and westward, owing to the presence of a similar submarine shelf surrounding the island. To test the behavior of the edge waves we simulated a fictitious event triggered in a bay located about 2 km southeast of the previous source. This shifted event, involving the same 0.0024-$km^3$ slide volume, produces a similar wave refraction and energy trapping, though wave heights higher than 3 m do not propagate far away (Figure 4c). The focusing area for this shifted source is shifted southward from Omoa Bay, so that maximal water heights do not exceed 1 m at Omoa (Figure 3b).

[13] These different computations show that the distance of focusing between the source and the site of highest onshore amplification essentially depends on the distance between the source and the shelf break. It is noteworthy that the EW prolongation of the submarine coastal shelf (<200 m deep) located at about 10°32′S does not influence the focusing of the tsunami waves. Preliminary test computations carried out without this bathymetric high did not change the results.

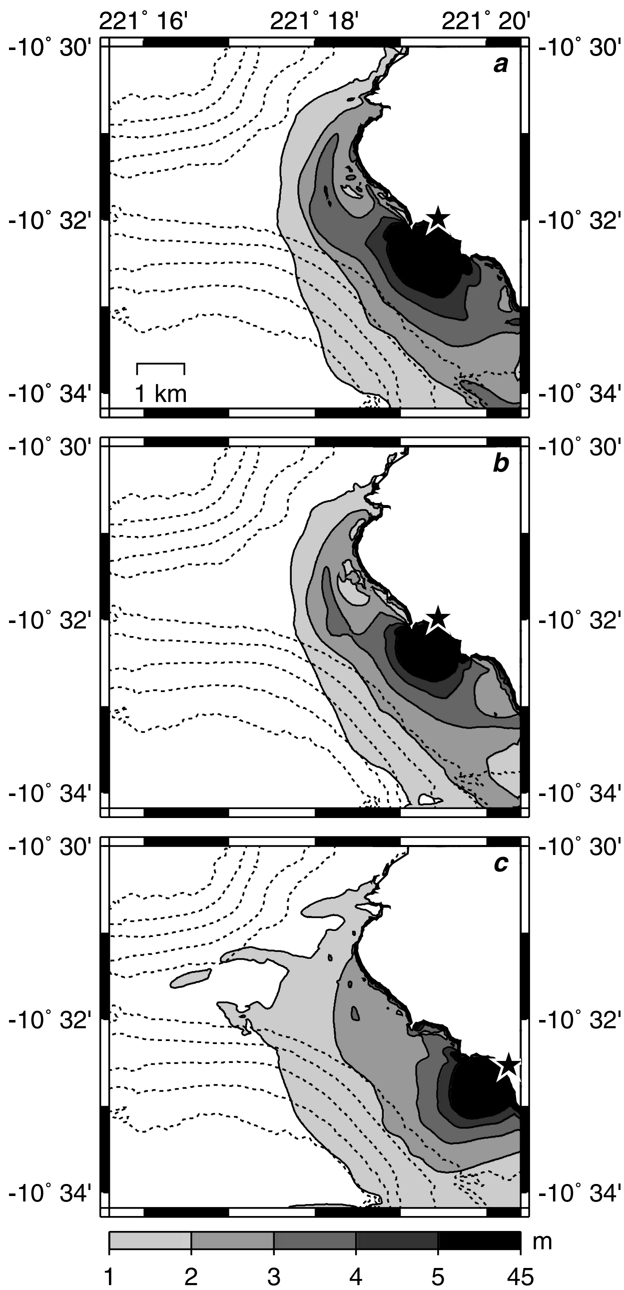


**Figure 4.** Maximal water heights are shown after an 8-min modeling time, for the 0.0024-$km^3$ event (a), the 0.0012-$km^3$ event (b), and the 0.0024-$km^3$ shifted event (c) (in this case, the longitudinal extent of the computational domain has been increased). Note that the gray scale is not linear to deal with high values reached around the area of failure. Dashed lines are the bathymetric values contoured at 200 m intervals.

[14] The trapping of waves around islands has been recently evoked for tsunamis induced by earthquakes, showing in particular amplification on the lee side of the island, with respect to the direction of propagation. Observations and results of laboratory experiments [*Yeh et al.*, 1994] as well as numerical modeling [*Piatanesi and Tinti*, 1998] contributed to evidence and demonstrate such phenomena. The behavior of the waves depends on their spectral characteristics and on the bathymetric profiles. However these studies dealt with long waves due to seismological sources located offshore. We show here a trapping of higher frequency waves induced by a landslide located onshore, that results in a significant inundation. In addition, edge waves are expected to be generated all the more efficiently as their source is located closer to the shoreline [*Mysak*, 1980].

[15] Numerous signs of previous cliff collapses have been reported on Fatu Hiva, that may have already triggered similar local tsunamis. These tsunamis are not directly related to active volcanic eruptions, but they can result in substantial damage with respect to the size of their source. The growth of coastal settlements in recent decades has significantly increased their associated hazards, as is the case in the Norwegian fjords [*Harbitz et al.*, 1993] and in other volcanic islands [*Tinti et al.*, 2000]. In light of our results, the assessment of such hazards can be realistically refined through adequate hydrodynamic numerical modelings, provided the bathymetry is known around the island and in the first tens of meters onshore. Along threatened shores of islands and continents, source areas potentially dangerous to inhabited sites could be defined and their hazards mitigated. Such an approach has been undertaken on a larger scale for Southern California coastal sites threatened by submarine landslides which could possibly trigger locally devastating tsunamis [*Borrero et al.*, 2001].

## 4. Conclusions

[16] The 1999 tsunami in Fatu Hiva (Marquesas Islands, French Polynesia) has been successfully simulated through our numerical model of the landslide as a fluid-like flow followed by a tsunami. Our results confirm that the cliff failure identified during the post-event survey can have triggered the 2- to 5-m high tsunami waves reported in Omoa Bay, with an initial volume of 0.0024 $km^3$ in agreement with gathered observations. We evidence a trapping of the waves on the coastal shelf, less than 200 m deep, that results in a particular focusing of the energy towards Omoa Bay. Considering this topographic trapping of the waves, the 1999 event occurred in a source area of particular danger to Omoa Bay. Our validated numerical model should allow us to improve the mitigation of such local tsunami hazards through relevant simulations in other potentially threatened coastal areas.

[17] **Acknowledgments.** EAO thanks his partners in the October 1999 field survey, as well as the people of Fatu Hiva for their warm welcome, especially Mayor T. Kamia and Mrs L. Kamia, the heroic school principal. The logistical support of Haut-Commissariat de la République is also acknowledged. We are grateful to both anonymous reviewers who allowed us to improve the discussion on our numerical model.

## References

Alcrudo, F., and P. Garcia-Navarro, A high-resolution Godunov-type scheme in finite volumes for the 2D shallow water equations, *Int. J. for Num. Meth. in Fluids*, *16*, 489–505, 1993.

Assier-Rzadkiewicz, S., et al., Numerical modelling of a landslide-generated tsunami: The 1979 Nice event, *Pure Appl. Geophys.*, *157*, 1707–1727, 2000.

Borrero, J. C., J. F. Dolan, and C. E. Synolakis, Tsunamis within the eastern Santa Barbara channel, *Geophys. Res. Lett.*, *28*, 643–646, 2001.

Fryer, G. J., E. A. Okal, J. C. Borrero, and C. Ruscher, Field report on the Fatu Hiva landslide and tsunami, 13 September 1999 (Abstract), *EOS Trans. Amer. Geophys. U.*, *81*, WP160, 2000.

Guibourg, S., P. Heinrich, and R. Roche, Numerical modeling of the 1995 Chilean tsunami, Impact on French Polynesia, *Geophys. Res. Lett.*, *24*, 775–778, 1997.

Harbitz, C. B., G. Pedersen, and B. Gjevik, Numerical simulations of large water waves due to landslides, *J. Hydraul. Eng.*, *119*, 1325–1342, 1993.

Hébert, H., P. Heinrich, F. Schindelé, and A. Piatanesi, Far-field simulation of tsunami propagation in the Pacific Ocean: Impact on the Marquesas Islands (French Polynesia), *J. Geophys. Res.*, *106*(C5), 9161–9177, 2001.

Heinrich, P., F. Schindelé, S. Guibourg, and P. Ihmlé, Modeling of the February 1996 Peruvian tsunami, *Geophys. Res. Lett.*, *25*, 2687–2690, 1998a.

Heinrich, P., A. Mangeney, S. Guibourg, R. Roche, G. Boudon, and J.-L. Cheminée, Simulation of water waves generated by a potential debris avalanche in Montserrat, Lesser Antilles, *Geophys. Res. Lett.*, *25*, 3697–3700, 1998b.

Heinrich, P., A. Piatanesi, E. Okal, and H. Hébert, Near-field modeling of the July 17, 1998 event in Papua New Guinea, *Geophys. Res. Lett.*, *27*, 3037–3040, 2000.

Heinrich, P., A. Piatenesi, and H. Hébert, Numerical modelling of tsunami generation and propagation from submarine slumps: The 1998 Papua New Guinea event, *Geophys. J. Int.*, *145*, 97–111, 2001a.

Heinrich, P., G. Boudon, J. C. Komorowski, R. S. J. Sparks, R. Herd, and B. Voight, Numerical simulation of the December 1997 debris avalanche in Montserrat, Lesser Antilles, *Geophys. Res. Lett.*, *28*, 2529–2532, 2001b.

Jiang, L., and P. Leblond, The coupling of a submarine slide and the surface waves it generates, *J. Geophys. Res.*, *97*, 731–744, 1992.

Mangeney, A., Ph. Heinrich, and R. Roche, Analytical solution for testing debris avalanche numerical models, *Pure Appl. Geophy.*, *157*, 1081–1096, 2000.

Mysak, L. A., Topographically trapped waves, *Ann. Rev. Fluid Mech.*, *12*, 45–76, 1980.

Piatanesi, A., and S. Tinti, Finite-element numerical simulations of tsunamis generated by earthquakes near a circular island, *Bull. Seismol. Soc. Am.*, *88*, 609–620, 1998.

Rabinovich, A. B., et al., The landslide-generated tsunami of November 3, 1994 in Skagway Harbor, Alaska: A case study, *Geophys. Res. Lett.*, *26*, 3009–3012, 1999.

Savage, S., and K. Hutter, The motion of a finite mass of granular material down a rough incline, *J. Fluid Mech.*, *199*, 177–215, 1989.

Tinti, S., E. Bortolucci, and A. Armigliato, Numerical simulation of the landslide-induced tsunami of 1988 in Vulcano Island, *Italy, Bull. Volcanol.*, *61*, 121–137, 1999.

Tinti, S., E. Bortolucci, and C. Romagnoli, Computer simulations of tsunamis due to sector collapse at Stromboli, Italy, *J. Volcanol. Geotherm. Res.*, *96*, 103–128, 2000.

Titov, V. V., and C. E. Synolakis, Modeling of breaking and non breaking long-wave evolution and runup using VTSC-2, *J. Wtrwy, Port, Coast. and Oc. Engrg*, *121*, 308–316, 1995.

Voight, B., Rockslides and avalanches, 2, Engineering Sites, Developments in Geotechnical Engineering, Vol. 14B, edited by B. Voight, Elsevier Scientific Publishing Company, 1979.

Yeh, H., P. Liu, M. Briggs, and C. Synolakis, Propagation and amplification of tsunamis at coastal boundaries, *Nature*, *372*, 353–355, 1994.

H. Hébert, P. Heinrich, and F. Schindelé, Laboratoire de Détection et de Géophysique, CEA, BP12, Bruyères-le-Châtel, 91680 France. (hebert@dase.bruyeres.cea.fr)

A. Piatanesi, Istituto Nazionale di Geofisica e Vulcanologia, Via di Vigna Murata, 605, 00143 Roma, Italy.

E. A. Okal, Department of Geological Sciences, Northwestern University, Evanston, IL 60208, USA.